European Radiology (2019) 29:6750–6761
https://doi.org/10.1007/s00330-019-06295-5

MOLECULAR IMAGING

Alterations of white matter network in patients with left and right non-lesional temporal lobe epilepsy

Yunli Yu[1,2] · Lan Chu[2,3] · Chunfeng Liu[1,3] · Mingming Huang[4] · Houfen Wang[2]

Received: 19 November 2018 / Revised: 7 May 2019 / Accepted: 29 May 2019 / Published online: 8 July 2019

Abstract

Objectives The goal of this study was to investigate alterations of white matter (WM) network in patients with left non-lesional temporal lobe epilepsy (nl-TLE) and right nl-TLE to assess the relationship between the white matter network properties and clinical parameters.

Methods T1 magnetic resonance imaging (MRI) and diffusion tensor imaging (DTI) were acquired for 45 participants, including 30 nl-TLE patients (13 left, 17 right) and 15 healthy controls. Diffusion tensor tractography was computed to model the WM structural network. The topologic properties of the WM network were obtained by graph theoretical analysis, and the between-group differences in global and nodal properties of the WM network were examined by network-based statistical analysis (NBS). The relationship between WM network properties and clinical parameters was assessed by Pearson's correlation analysis.

Results NBS results indicated that patients with left and right nl-TLE experienced distinct changes of WM nodal and global network properties compared with HCs. Positive correlation coefficients were found in several regions. The structural disruptions of networks in the two nl-TLE groups were observed to be different in distribution and severity.

Conclusions This study provides evidence for changes of the WM network topological properties and structural connectivity in nl-TLE patients, which provide useful insights for the understanding of disease mechanisms of TLE and improving treatment outcomes for nl-TLE.

Key Points

- *This study aims to investigate alterations of white matter (WM) network in patients with non-lesional temporal lobe epilepsy (nl-TLE).*
- *Network-based statistical analysis results indicated that patients with left and right nl-TLE experienced distinct changes of WM nodal and global network properties compared with healthy controls.*
- *This study provides useful insights for the understanding of disease mechanisms of TLE and improving treatment outcomes for nl-TLE.*

Keywords Non-lesional temporal lobe epilepsy · White matter network · Diffusion tensor tractography · Graph theory

✉ Lan Chu
chulan8999@yeah.net

[1] Department of Neurology, The Second Affiliated Hospital of Soochow University, Suzhou 215004, Jiangsu, China

[2] Department of Neurology, The Affiliated Hospital of Guizhou Medical University, No.28 Guiyi Street, Guiyang 550004, Guizhou, China

[3] Department of Neurology, Institute of Neuroscience, Soochow University, Suzhou 215123, Jiangsu, China

[4] Department of Image, The Affiliated Hospital of Guizhou Medical University, Guiyang 550004, Guizhou, China

Abbreviations

AMYG	Amygdala
BNT	Boston Naming Test
DTI	Diffusion tensor imaging
DSST	Digit symbol substitution test
EEG	Electroencephalogram
FA	Fractional anisotropy
FACT	Fiber assignment by continuous tracking
FOV	Field of view
HAMD	Hamilton Depression Scale
HCs	Healthy controls
HS	Hippocampal sclerosis
MMSE	Mini-mental state examination
MNI	Montreal Neurological Institute

MOCA	Montreal Cognitive Assessment
MRI	Magnetic resonance imaging
mTLE	Mesial TLE
nl-TLE	Non-lesional temporal lobe epilepsy
PCG.	Posterior cingulate gyrus
SFGdor.	Superior frontal gyrus (dorsolateral)
SPG.	Superior parietal gyrus
TBSS	Tract-based spatial statistics method
TE	Echo time
TLE	Temporal lobe epilepsy
TR	Repetition time
WM	White matter

Introduction

Temporal lobe epilepsy (TLE) is one of the most common localization-related epilepsy syndromes. Structural and functional abnormalities could be found both within and beyond the ictal onset zone and the effected ipsilateral hippocampus [1]. Non-lesional temporal lobe epilepsy (nl-TLE), consisting of up to 30% all TLE cases, is an important TLE subgroup with normal (or negative) magnetic resonance imaging (MRI) findings [2]. Different from common TLE cases, nl-TLE patients do not show evidence of hippocampal sclerosis (HS) and are absent from visible epileptogenic lesions in MRI examination, which inevitably increases the difficulty for diagnosis and therapy. Compared with patients with HS, nl-TLE patients have been observed to have delayed onset of epilepsy [3], lower prevalence of febrile convulsions [4], less impairment of memory function [5], and worse surgical outcomes [6]. Differences in disease symptoms suggest that certain brain abnormalities may be selective to patients with nl-TLE, and it is noteworthy to use neuroimaging techniques to study nl-TLE.

A previous study demonstrated that from the viewpoint of epileptic genesis and seizure propagation, TLE can be modeled as a network disorder that affects large neural networks that are closely associated with brain functions [7]. White matter (WM) fiber connections derived from diffusion tensor imaging (DTI) tractography is a useful tool to study structural connections. Previous mesial TLE (mTLE) study has found structural and functional abnormalities within the default mode network of the mesial TLE, suggesting that TLE may be the consequence of the degeneration of structural connectivity due to the reduced connection density [8]. Mesial TLE has been associated with loss of nerve fibers and abnormal increase in structural connectivity of limbic structures [9]. The individual connections in the whole brain connectivity matrix in patients with TLE were also examined [10]. The alteration in the topologic characteristics of a whole brain white matter network in a group of mesial TLE patients was calculated and patients exhibited global and local efficiency decreases and regional efficiency generally decreases in the ipsilateral temporal, bilateral frontal, and bilateral parietal areas [11]. These results provided evidence of disruption of brain structural circuits in patients with TLE.

Clinical observations and selective studies suggested that the localization of seizure is a key factor, which might contribute to different symptoms and surgical outcomes. For example, Pustina et al compared left TLE and right TLE patients with healthy controls (HCs), concluding that left TLE patients had more severe losses in structural orientation and more altered correlations with pathologic processes [12]. Study of WM alterations in nl-TLE patients also suggested that left nl-TLE and their siblings showed more WM abnormalities [13].

Based on these findings and suggestions, our study proposed to investigate the alterations of WM network topologic properties in the global and nodal level. We hypothesized that similar to TLE, left and right nl-TLE would show distinct changes in WM networks. By analyzing network abnormalities in left and right nl-TLE patients compared to HCs and examining the correlations between network properties and cognitive function scores, we aimed to better understand cognitive impairments due to localization-related epilepsy.

Materials and methods

Subjects

In this study, 45 right-handed participants were involved, including 30 nl-TLE patients (13 left, 17 right) and 15 age-, gender-, and education-matched healthy control subjects. The patients were recruited from the Epilepsy of the Clinic of Department of Neurology of the Affiliated Hospital of Guizhou Medical University. The control subjects were recruited by advertisement. Each participant was assessed by a standard clinical evaluation protocol, which comprised the Montreal Cognitive Assessment (MOCA), the Boston Naming Test (BNT), the digit symbol substitution test (DSST), and Rey Auditory Verbal Learning Test (RAVLT). Detailed demographics and clinical characteristics of the participants of each subject group were presented in Table 1.

The inclusion and exclusion criteria in this study can be summarized as the following points: participants would be included if (1) the clinical onset of symptoms showed the location of epileptogenic focus in the temporal lobe; (2) no seizure was observed within 24 h before MRI scanning; (3) electroencephalogram (EEG) video-telemetry demonstrated unilateral temporal lobe ictal onset; (4) no lesions were visually identified on the clinical imaging; (5) disease duration was longer than 1 year; and (6) age ranges from 16 to 75;

Table 1 Participant demographics and neuropsychological test scores

	Left nl-TLE ($n = 13$)	Right nl-TLE ($n = 17$)	Controls ($n = 15$)	F value/ χ^2	p value
Age (years)	28.92 ± 12.55	33.29 ± 14.26	32.00 ± 10.81	0.447	0.643
Gender M/F	6/7	8/9	7/8	0.0011	0.998
Education (years)	11.50 ± 3.38	10.18 ± 2.51	11.80 ± 3.86	1.108	0.340
Duration of TLE	5.89 ± 6.30	7.03 ± 8.04	–	0.182	0.671
Effective medication (n)	8	6	–		
MOCA	24.46 ± 3.66	24.11 ± 3.12	26.93 ± 2.25	3.896	0.028[a,b]
Boston Naming Test	18.77 ± 2.89	17.88 ± 3.79	22.53 ± 3.23	8.29	0.001[a,b]
DSST	51.38 ± 10.18	44.64 ± 7.30	57.40 ± 10.08	7.762	0.001[b]
RAVLT	46.46 ± 12.03	41.52 ± 10.70	52.60 ± 7.74	4.657	0.015[a,b]
RAVLT delayed recall	8.92 ± 3.27	7.65 ± 3.85	11.80 ± 2.14	6.896	0.003[a,b]

Values are represented as the mean ± SD. Using χ^2 test for gender, and ANOVA group tests for age and years of education, no significant group difference was observed. NS indicates non-significance ($p > 0.05$)

[a] Post hoc comparison results show significant group differences between left nl-TLE and HCs

[b] Post hoc comparison results show significant group differences between right nl-TLE and HCs

MOCA, Montreal Cognitive Assessment; *DSST*, digit symbol substitution test; *RAVLT*, Rey Auditory Verbal Learning Test

participants would be excluded if (1) they were left-handed; (2) scored ≤ 24 in the mini-mental state examination (MMSE); (3) scored > 20 in the Hamilton Depression Scale (HAMD); (4) had history of psychiatric or neurological disorders; (5) had history of physical illness and prior head injury; (6) had history of alcoholism and drug abuse; and (7) currently on any medications that may affect cognitive functioning for MRI scanning.

This study was approved by the research ethics board of the Affiliated Hospital of Guizhou Medical University and complied with the Declaration of Helsinki. Prior to this study, all of the patients and the healthy controls received a complete description about this experiment, and informed consent was obtained from each participant in written form.

Data acquisition

High-resolution 3D T1-weighted images were acquired on a 3-T MRI machine (Philips Achieva) with the following acquisition parameters: repetition time (TR) = 12 ms, echo time (TE) = 6 ms, field of view (FOV) = 250 mm × 250 mm, recon voxel size = 0.6 × 0.6 × 0.6 mm^3, slice thickness = 1 mm, matrix = 416 × 227, and NSA = 1; all participants were instructed to stay still during the acquisition. Images with extensive motion artifact (greater than 2 mm or 2° rotation angle) were discarded. DTI was acquired by single-shot spin-echo planar imaging (TR = 6800 ms, TE = 70 ms, FOV = 200 mm × 200 mm, recon voxel size = 2 × 2 × 2 mm^3, matrix = 144 × 144, slice thickness = 2 mm, NSA = 2, gap = 0 mm).

T1 and DTI data preprocessing

Data preprocessing was performed with the MATLAB toolbox PANDA_1.3.1_64 (https://www.nitrc.org/projects/panda/). In this study, the raw dataset was composed of two types of images: diffusion tensor images (DTI) and T1-weighted structural images (T1), which should be handled in different steps.

DTIs were preprocessed with the following steps: (1) The diffusion images were corrected by applying the affine transform of each image to the b = 0 image, in order to avoid the distortion caused by eddy currents and head motion. (2) A skull removal process was applied to split the non-brain tissues and background noise from the corrected images. (3) Fractional anisotropy (FA) maps were then calculated as quantitative diffusion tensor parameters to describe the distribution of the white matter (WM) fiber tracts in the whole brain.

Fig. 1 A flowchart for construction of WM networks based on topological analysis. (i) T1-weighted structural images and DTIs were preprocessed and registered to the MNI space. The WM fiber tracts were tracked by FACT algorithm. (ii) Brain regions were parcellated by AAL90 atlas and used to define nodes and edges. FA-weighted WM networks were then constructed in symmetric 90 × 90 matrix form. (iii) Network properties were calculated based on topological methods. (iv) FA skeletons were defined using TBSS method and were used to calculate mean FA maps. Statistical analysis was applied to seek out significant between-group differences. MRI, magnetic resonance imaging; DTI, diffusion tensor image; WM, white matter; FACT, fiber assignment by continuous tracking; AAL90, automated anatomical labeling atlas with 90 brain regions; FA, fractional anisotropy; TBSS, tract-based spatial statistics

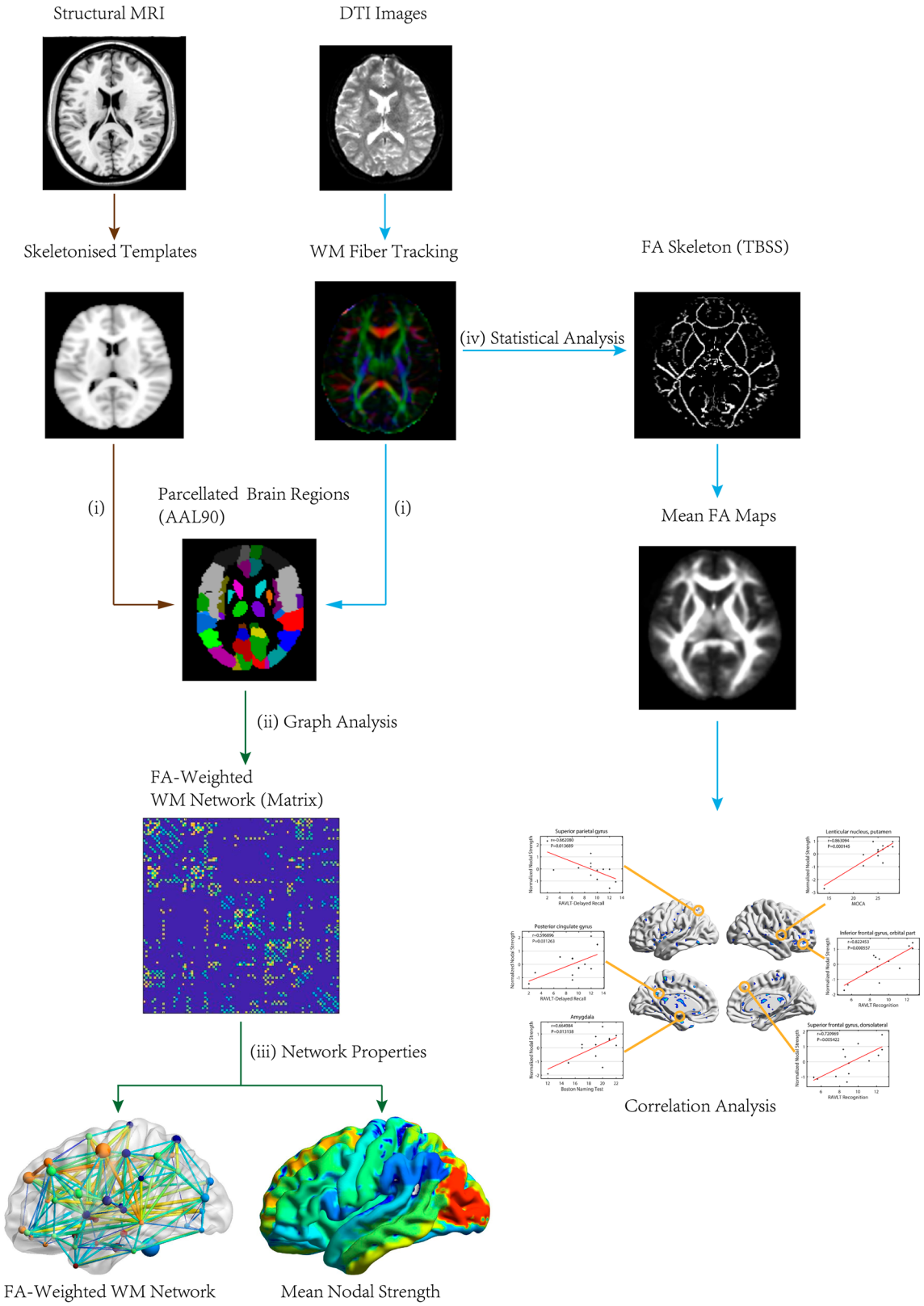

T1-weighted structural images would be used as the templates of brain regions in the data analysis procedure. In this study, T1 images were standardized and non-linearly transformed into the Montreal Neurological Institute (MNI) space, using the ICBM152 T1 template as a reference.

Network construction

In this study, brain networks were constructed at the macroscale, where nodes represented brain regions and edges represented connections between two nodes. The general process of WM network construction and graph analysis is illustrated in Fig. 1. WM network fiber tracts were tracked using the "fiber assignment by continuous tracking" (FACT) algorithm in PANDA toolbox [14]. Therefore, those adjacent voxels, of which the FA metrics were > 0.2, would be considered to be at the same tract. Diffusion tensor tractography was then computed. The skeleton of WM network fiber tracts was defined using the tract-based spatial statistics (TBSS) method in the PANDA toolbox and was used to calculate the mean FA maps as the preparation for further statistical analysis [15]. The nodes and edges defined were referred to the automated anatomical labeling atlas with 90 brain regions (AAL90) [16]. As a result, we constructed the FA-weighted WM network which was presented as a symmetric 90 × 90 matrix.

Network analysis

On the basis of the topological method, both global and nodal metrics were calculated to characterize the constructed FA-weighted brain network for each subject. The analysis procedure was carried out by using the GRETNA toolbox (https://www.nitrc.org/projects/gretna/). Global network metrics included small world property (clustering coefficient Cp, and shortest path length Lp, normalized clustering coefficient γ, normalized characteristic path length λ, and small-worldness σ) and global network efficiency (global efficiency and local efficiency). Typically, a small-world network shows $\gamma > 1$ and $\lambda \approx 1$, which means it will be significantly more clustered than the surrogate random networks with similar shortest path length [17]. The global efficiency measures the effectiveness of parallel information transfer in the global network, and the local efficiency reveals the fault tolerance of the network [18]. Nodal network metrics included betweenness centrality, degree centrality, nodal clustering coefficient, nodal efficiency, nodal local efficiency, and nodal shortest path. Especially, the nodal degree centrality was defined as the number of links to a certain nod [19], and it was employed as the nodal strength in this study.

Statistical analysis

Between-group differences in topologic network attributes were detected by the network-based statistic (NBS) method with three steps. Firstly, a one-way analysis of variance test (ANOVA) was applied on the FA-weighted networks (in a symmetric 90 × 90 matrix form) to seek out nodes with significant group difference ($p < 0.05$, corrected with FWER) in network metrics. Those nodes would be taken as regions in interests (ROIs). Then 2-sample *t* tests were performed as post hoc tests between every two groups (left nl-TLE vs. HCs; right nl-TLE vs. HCs) using the SPM12 toolbox (https://www.fil.ion.ucl.ac.uk/spm/).

Table 2 Group differences in global properties among left nl-TLE, right nl-TLE, and HCs

Network metric		Subjects			Group ANOVA		Post hoc *t* test	
		Left nl-TLE	Right nl-TLE	HC	*p* value	*F* score	HC vs. L	HC vs. R
Small-worldness	Cp	0.263 (0.016)	0.263 (0.023)	0.261 (0.014)	0.761	0.275	n.s.	n.s.
	Cp′	0.082 (0.009)	0.086 (0.012)	0.083 (0.007)	–	–	–	–
	Lp	5.664 (0.331)	5.809 (0.434)	5.530 (0.306)	0.004	6.462	HC < L	HC < R
	Lp′	5.246 (0.288)	5.384 (0.387)	5.116 (0.260)	–	–	–	–
	γ	3.229 (0.299)	3.094 (0.259)	3.161 (0.220)	–	–	–	–
	λ	1.080 (0.013)	1.079 (0.012)	1.081 (0.016)	–	–	–	–
	σ	2.988 (0.263)	2.868 (0.229)	2.923 (0.184)	–	–	–	–
Global efficiency	Eg	0.078 (0.004)	0.076 (0.005)	0.080 (0.004)	0.008	5.483	HC > L	HC > R
	Eloc	0.104 (0.005)	0.103 (0.007)	0.106 (0.005)	0.018	4.457	HC > L	HC > R

The statistic results of global metrics are presented in the table (mean (SD)). Group ANOVA test was performed to detect group differences ($p < 0.05$), followed by post hoc 2-sample *t* test between two groups ($p < 0.05$, corrected with FWER). Age, gender, and education were taken as covariates in the statistical analysis and removed by introducing multiple regression model

The small-worldness metric includes global clustering coefficient (Cp), global clustering coefficient of surrogate random networks (Cp′), global shortest path length (Lp), global shortest path length of surrogate random networks (Lp′), gamma (γ), lambda (λ), and sigma(σ). $\gamma = Cp/Cp'$, $\lambda = Lp/Lp'$, $\sigma = \gamma/\lambda$. Networks with small-worldness should be observed to have $\gamma > 1$, $\lambda \approx 1$, and $\sigma >> 1$

The global efficiency metric includes global efficiency (Eg) and local efficiency (Eloc)

n.s, no significance was found

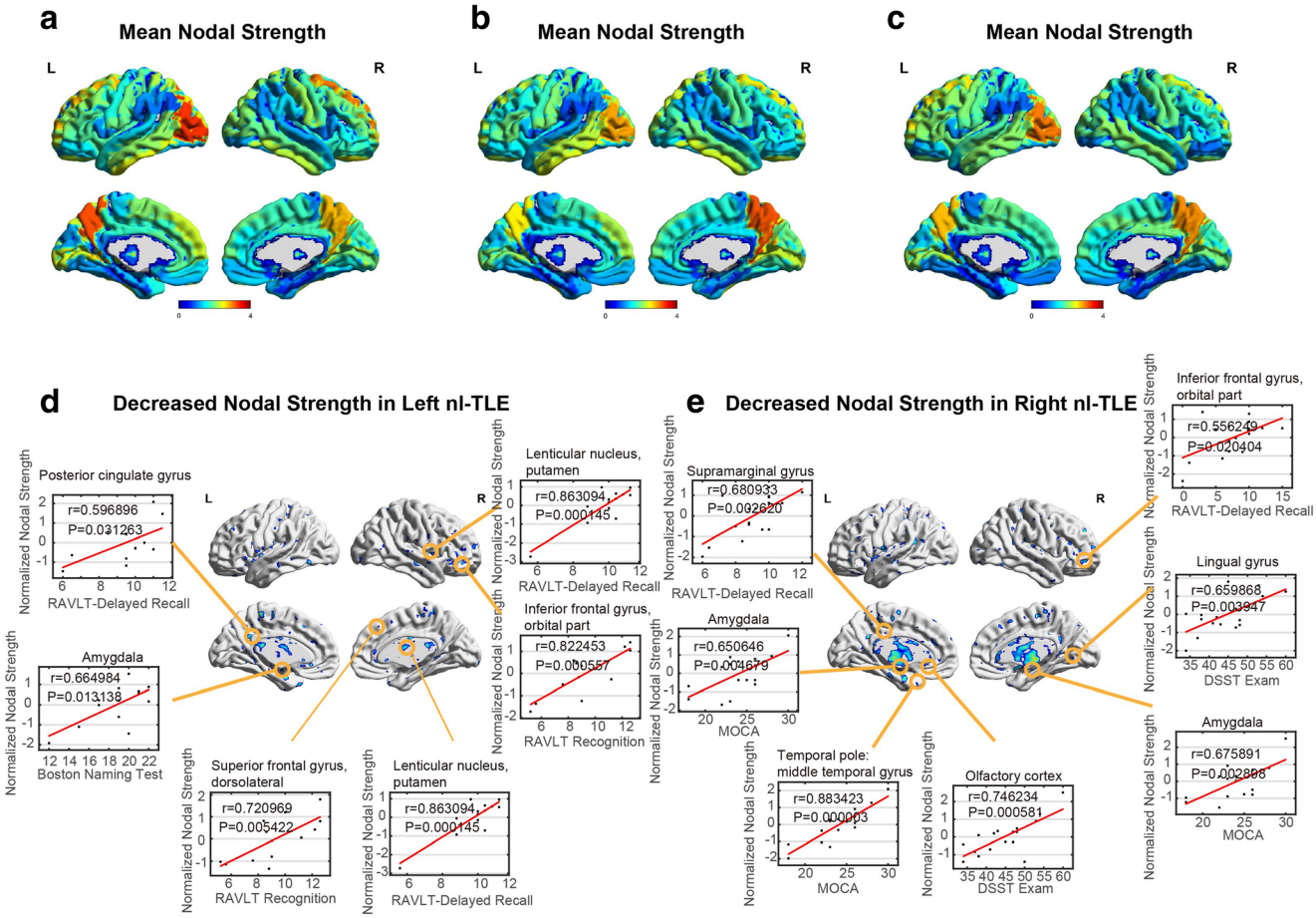

Fig. 2 Distribution of mean nodal strength and regions with significant differences. Distribution of mean nodal strength in the healthy control (HC) subjects (**a**), left nl-TLE subjects (**b**), right nl-TLE subjects (**c**), and between-group differences (**d**), left nl-TLE < HC and right nl-TLE < HC (**e**). The significance of the p value < 0.05 was corrected by the family-wise error rate (FWER) test. Brain regions with significantly decreased nodal strength were taken as regions of interest (ROIs). Pearson correlation analysis was conducted between those ROIs and the clinical recognition test scores (with age, gender, and education as covariates). Nodes weighted by nodal strength were mapped onto the cortical surfaces using the BrainNet Viewer toolbox (https://www.nitrc.org/projects/bnv/). MOCA, Montreal Cognitive Assessment; BNT, Boston Naming Test; DSST, digit symbol substitution test; RAVLT, Rey Auditory Verbal Learning Test

Age, gender, and education were treated as covariates in all steps of the statistical analysis. The effects of those covariates were removed by introducing the multiple linear regression model. The whole procedures were completed by MATLAB Statistics and Machine Learning Toolbox (https://www.mathworks.com/products/statistics.html). To present the results in the form of images, nodes and FA-weighted edges with altered properties were plotted using the BrainNet Viewer toolbox (https://www.nitrc.org/projects/bnv/).

Correlation assessment were conducted between FA-weighted WM network properties (the clustering coefficient, small world parameters (γ, λ, σ), shortest path length, global network efficiency, and local network efficiency) and cognitive assessment scores (Montreal Cognitive Assessment, Boston Naming Test, digit symbol substitution test, Rey Auditory Verbal Learning Test, and word fluency test) in the ROIs of patients with left nl-TLE and right nl-TLE.

Results

Demographic and clinical characteristics

The demographic information in this study is listed in Table 1. There were no significant differences found in age, gender, or education among the three groups (all $p > 0.34$). The nl-TLE groups (left and right) had significantly lower scores on the MOCA ($p = 0.0281$), Boston Naming Test ($p = 0.0009$), DSST ($p = 0.0014$), RAVLT recognition ($p = 0.0149$), and RAVLT delayed recall ($p = 0.0026$) than the HC group.

Global properties of the WM network

Both TLE patients and HCs were observed to have the small-world attributes ($\gamma > 1$, $\lambda \approx 1$, $\sigma >> 1$). According to ANOVA group test results (Table 2), compared with the HC group, significant decrease was found in the

Table 3 Brain regions with significant group differences in nodal properties among left nl-TLE, right nl-TLE, and HCs

Network metric	Brain region	Abbr.	Category	Coordinate (x, y, z)			Group ANOVA		Post hoc *t* test	
							p value	*F* score	HC vs. L	HC vs. R
Degree centrality (DC)	Temporal pole: middle temporal gyrus	TPOmid.R	Paralimbic	44.22	14.55	− 32.23	< 0.001	16.375	n.s.	HC > R
	Inferior frontal gyrus, orbital part	ORBinf.R	Paralimbic	41.22	32.23	− 11.91	< 0.001	10.581	HC > L	HC > R
	Lingual gyrus	LING.R	Association	16.29	− 66.93	− 3.87	0.001	9.017	HC > L	HC > R
	Superior frontal gyrus, dorsolateral	SFGdor.L	Association	− 18.45	34.81	42.2	0.002	7.046	HC > L	HC > R
	Precentral gyrus	PreCG.L	Primary	− 38.65	− 5.68	50.94	0.004	6.310	n.s.	HC > R
	Supramarginal gyrus	SMG.L	Association	− 55.79	− 33.64	30.45	0.009	5.270	HC > L	HC > R
	Olfactory cortex	OLF.L	Limbic	− 8.06	15.05	− 11.46	0.010	5.093	HC > L	HC > R
	Superior parietal gyrus	SPG.L	Association	− 23.45	− 59.56	58.96	0.010	5.089	HC > L	HC > R
	Superior temporal gyrus	STG.L	Association	− 53.16	− 20.68	7.13	0.012	4.970	n.s.	HC > R
	Superior frontal gyrus, dorsolateral	SFGdor.R	Association	21.9	31.12	43.82	0.013	4.860	HC > L	HC > R
	Lenticular nucleus, putamen	PUT.R	Subcortical	27.78	4.91	2.46	0.020	4.284	HC > L	n.s.
	Heschl gyrus	HES.R	Primary	45.86	− 17.15	10.41	0.020	4.274	n.s.	HC > R
	Middle occipital gyrus	MOG.L	Association	− 32.39	− 80.73	16.11	0.021	4.242	HC > L	HC > R
	Temporal pole: middle temporal gyrus	TPOmid.L	Paralimbic	− 36.32	14.59	− 34.08	0.025	4.016	n.s.	HC > R
	Amygdala	AMYG.L	Subcortical	− 23.27	− 0.67	− 17.14	0.025	4.013	HC > L	HC > R
	Posterior cingulate gyrus	PCG.L	Paralimbic	− 4.85	− 42.92	24.67	0.026	3.983	HC > L	HC > R
	Median cingulate and paracingulate gyri	DCG.R	Paralimbic	8.02	− 8.83	39.79	0.034	3.655	HC > L	n.s.
	Amygdala	AMYG.R	Subcortical	27.32	0.64	− 17.5	0.035	3.643	HC > L	HC > R
Betweenness centrality (BC)	Median cingulate and paracingulate gyri	DCG.R	Paralimbic	8.02	− 8.83	39.79	0.003	6.529	n.s.	HC > R
	Superior frontal gyrus, dorsolateral	SFGdor.R	Association	21.9	31.12	43.82	0.005	5.958	HC > L	HC > R
	Superior temporal gyrus	STG.L	Association	− 53.16	− 20.68	7.13	0.015	4.688	n.s.	HC > R
	Superior frontal gyrus, orbital part	ORBsup.L	Paralimbic	− 16.56	47.32	− 13.31	0.024	4.103	HC > L	n.s.
	Insula	INS.R	Paralimbic	39.02	6.25	2.08	0.025	4.015	n.s.	HC > R
	Temporal pole: superior temporal gyrus	TPOsup.L	Paralimbic	− 39.88	15.14	− 20.18	0.034	3.684	HC > L	n.s.
	Median cingulate and paracingulate gyri	DCG.L	Paralimbic	− 5.48	− 14.92	41.57	0.035	3.645	n.s.	HC > R
	Superior parietal gyrus	SPG.L	Association	− 23.45	− 59.56	58.96	0.042	3.412	HC > L	HC > R
Nodal clustering coefficient (NCp)	Anterior cingulate and paracingulate gyri	ACG.R	Paralimbic	8.46	37.01	15.84	< 0.001	9.217	n.s.	HC > R
	Superior frontal gyrus, orbital part	ORBsup.L	Paralimbic	− 16.56	47.32	− 13.31	0.002	7.526	HC > L	n.s.
	Posterior cingulate gyrus	PCG.R	Paralimbic	7.44	− 41.81	21.87	0.002	6.963	n.s.	HC > R
	Inferior frontal gyrus, orbital part	ORBinf.R	Paralimbic	41.22	32.23	− 11.91	0.007	5.528	HC > L	HC > R
	Heschl gyrus	HES.L	Primary	− 41.99	− 18.88	9.98	0.008	5.379	HC > L	HC > R
	Supplementary motor area	SMA.R	Association	8.62	0.17	61.85	0.013	4.837	HC > L	HC > R
	Lingual gyrus	LING.R	Association	16.29	− 66.93	− 3.87	0.015	4.687	HC > L	n.s.
	Olfactory cortex	OLF.R	Limbic	10.43	15.91	− 11.26	0.020	4.330	n.s.	HC > R
	Superior frontal gyrus, medial	SFGmed.R	Association	9.1	50.84	30.22	0.027	3.958	n.s.	HC > R
	Median cingulate and paracingulate gyri	DCG.R	Paralimbic	8.02	− 8.83	39.79	0.029	3.850	n.s.	HC > R
	Thalamus	THA.R	Subcortical	13	− 17.55	8.09	0.040	3.472	HC > L	HC > R
	Middle occipital gyrus	MOG.R	Association	37.39	− 79.7	19.42	0.049	3.246	HC > L	n.s.
	Superior parietal gyrus	SPG.L	Association	− 23.45	− 59.56	58.96	0.049	3.237	HC > L	n.s.
Nodal efficiency (Ne)	Inferior frontal gyrus, orbital part	ORBinf.R	Paralimbic	41.22	32.23	− 11.91	< 0.001	12.477	HC > L	HC > R
	Olfactory cortex	OLF.L	Limbic	− 8.06	15.05	− 11.46	0.002	7.373	n.s.	HC > R
	Temporal pole: middle temporal gyrus	TPOmid.R	Paralimbic	44.22	14.55	− 32.23	0.002	7.031	n.s.	HC > R
	Lingual gyrus	LING.R	Association	16.29	− 66.93	− 3.87	0.004	6.468	n.s.	HC > R
	Posterior cingulate gyrus	PCG.L	Paralimbic	− 4.85	− 42.92	24.67	0.004	6.316	HC > L	HC > R
	Amygdala	AMYG.R	Subcortical	27.32	0.64	− 17.5	0.006	5.735	n.s.	HC > R
	Amygdala	AMYG.L	Subcortical	− 23.27	− 0.67	− 17.14	0.008	5.463	HC > L	HC > R
	Middle frontal gyrus, orbital part	ORBmid.R	Paralimbic	33.18	52.59	− 10.73	0.011	5.040	n.s.	HC > R

Table 3 (continued)

Network metric	Brain region	Abbr.	Category	Coordinate (x, y, z)			Group ANOVA		Post hoc *t* test	
							p value	*F* score	HC vs. L	HC vs. R
	Superior parietal gyrus	SPG.L	Association	−23.45	−59.56	58.96	0.015	4.616	HC > L	HC > R
	Posterior cingulate gyrus	PCG.R	Paralimbic	7.44	−41.81	21.87	0.030	3.831	HC > L	HC > R
	Temporal pole: middle temporal gyrus	TPOmid.L	Paralimbic	−36.32	14.59	−34.08	0.032	3.755	n.s.	HC > R
	Superior frontal gyrus, medial orbital	ORBsupmed.L	Paralimbic	−5.17	54.06	−7.4	0.032	3.736	HC > L	HC > R
	Superior frontal gyrus, dorsolateral	SFGdor.R	Association	21.9	31.12	43.82	0.032	3.723	n.s.	HC > R
	Fusiform gyrus	FFG.R	Association	33.97	−39.1	−20.18	0.033	3.703	n.s.	HC > R
	Supramarginal gyrus	SMG.L	Association	−55.79	−33.64	30.45	0.043	3.388	HC > L	HC > R
	Middle frontal gyrus, orbital part	ORBmid.L	Paralimbic	−30.65	50.43	−9.62	0.045	3.338	HC > L	HC > R
Nodal local efficiency (Nle)	Superior frontal gyrus, orbital part	ORBsup.L	Paralimbic	−16.56	47.32	−13.31	0.002	6.988	HC > L	n.s.
	Heschl gyrus	HES.R	Primary	45.86	−17.15	10.41	0.003	6.726	n.s.	HC > R
	Heschl gyrus	HES.L	Primary	−41.99	−18.88	9.98	0.003	6.582	HC > L	HC > R
	Superior parietal gyrus	SPG.L	Association	−23.45	−59.56	58.96	0.004	6.384	HC > L	HC > R
	Anterior cingulate and paracingulate gyri	ACG.R	Paralimbic	8.46	37.01	15.84	0.005	6.135	n.s.	HC > R
	Posterior cingulate gyrus	PCG.R	Paralimbic	7.44	−41.81	21.87	0.012	4.926	HC > L	n.s.
	Temporal pole: middle temporal gyrus	TPOmid.R	Paralimbic	44.22	14.55	−32.23	0.014	4.723	HC > L	n.s.
	Supplementary motor area	SMA.L	Association	−5.32	4.85	61.38	0.017	4.485	HC > L	n.s.
	Supplementary motor area	SMA.R	Association	8.62	0.17	61.85	0.020	4.285	HC > L	n.s.
	Superior frontal gyrus, medial	SFGmed.R	Association	9.1	50.84	30.22	0.021	4.215	HC > L	HC > R
	Inferior temporal gyrus	ITG.R	Association	53.69	−31.07	−22.32	0.026	4.002	HC > L	n.s.
	Fusiform gyrus	FFG.L	Association	−31.16	−40.3	−20.23	0.031	3.767	n.s.	HC > R
	Olfactory cortex	OLF.R	Limbic	10.43	15.91	−11.26	0.033	3.703	n.s.	HC > R
Nodal shortest path length (NLp)	Lingual gyrus	LING.R	Association	16.29	−66.93	−3.87	0.009	5.363	n.s.	HC > R
	Superior parietal gyrus	SPG.L	Association	−23.45	−59.56	58.96	0.021	4.237	HC > L	HC > R
	Gyrus rectus	REC.L	Paralimbic	−5.08	37.07	−18.14	0.027	3.950	n.s.	HC > R
	Amygdala	AMYG.L	Subcortical	−23.27	−0.67	−17.14	0.031	3.885	HC > L	HC > R
	Superior frontal gyrus, dorsolateral	SFGdor.R	Association	21.9	31.12	43.82	0.035	3.639	n.s.	HC > R
	Superior frontal gyrus, medial	SFGmed.L	Association	−4.8	49.17	30.89	0.040	3.472	n.s.	HC > R
	Precuneus	PCUN.L	Association	−7.24	−56.07	48.01	0.045	3.355	HC > L	HC > R

Group ANOVA test was performed to detect group differences ($p < 0.05$), followed by post hoc 2-sample *t* test between two groups ($p < 0.05$, corrected with FWER). Age, gender, and education were treated as covariates in the statistical analysis by introducing multiple regression model. Nodal property measurements include degree centrality (DC), betweenness centrality (BC), nodal clustering coefficient (NCp), nodal efficiency (Ne), nodal local efficiency (Nle), and nodal shortest path (NLp). Brain regions were parcellated and nodes were defined based on AAL90 atlas

global network efficiency (HC 0.0802 ± 0.0042; left nl-TLE 0.0783 ± 0.0042; right nl-TLE 0.0764 ± 0.0054; $p = 0.0077$) and the local network efficiency (HC 0.1063 ± 0.0050; left nl-TLE 0.1044 ± 0.0047; right nl-TLE 0.1025 ± 0.0068; $p = 0.0176$), and significant increase was found in the shortest path length (HC 5.5299 ± 0.3057; left nl-TLE 5.6673 ± 0.3308; right nl-TLE 5.8089 ± 0.4344; $p = 0.0036$). No significance was found in the global clustering coefficient ($p = 0.7610$).

Nodal properties of the WM network

Distribution of mean nodal strength was basically similar in HC, left nl-TLE, and right nl-TLE groups (Fig. 2a–c). However, significant group differences ($p < 0.05$, FWER corrected) in nodal properties were found in some nodes (Fig. 2d, e). The coordinates, abbreviations, and corresponding correlation coefficients of these regions were listed in Table 3. Nodal strengths of patients with left nl-TLE were found to be significantly decreased in the right inferior frontal gyrus (orbital part) (ORBinf.R), left superior frontal gyrus (dorsolateral) (SFGdor.L), left supramarginal gyrus (SMG.L), left superior parietal gyrus (SPG.L), left amygdala (AMYG.L), and left posterior cingulate gyrus (PCG.L). Nodal strengths of patients with right nl-TLE were found to be significantly decreased in the right temporal pole: middle temporal gyrus (TPOmid.R), right inferior frontal gyrus (orbital part)

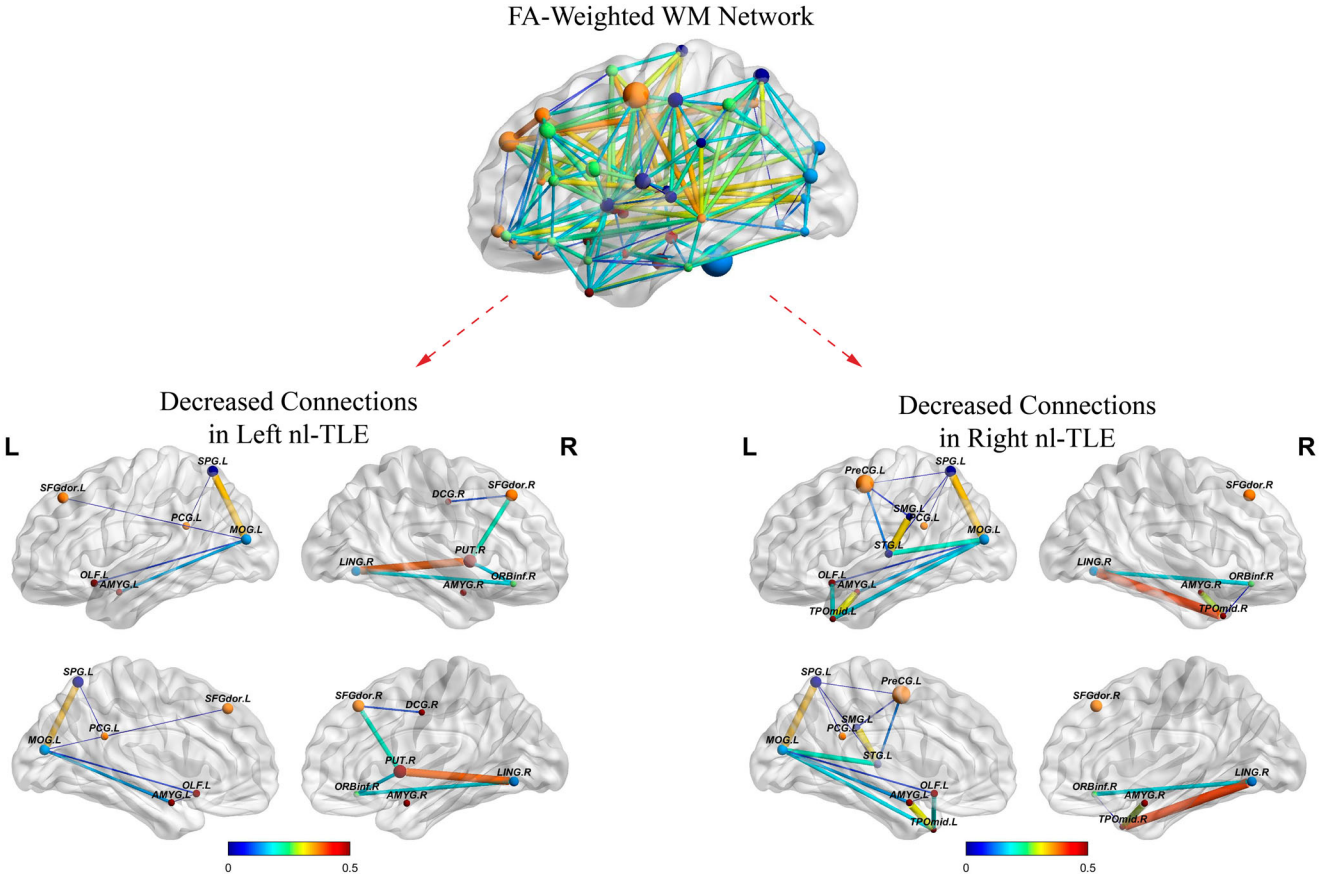

Fig. 3 Decreased connections in patients with non-lesional temporal lobe epilepsy (nl-TLE)

(ORBinf.R), right lingual gyrus (LING.R), left supramarginal gyrus (SMG.L), left olfactory cortex (OLF.L), middle occipital gyrus (MOG.L), left temporal pole: middle temporal gyrus (TPOmid.L), left amygdala (AMYG.L), left posterior cingulate gyrus (PCG.L), and right amygdala (AMYG.R). Those nodes were taken as regions in interest. The decreased connections in the nl-TLE groups were illustrated in Fig. 3, using the NBS method. The disrupted connections were mainly distributed in the association network (7/18 nodes) and the paralimbic network (5/18 nodes).

Relationship between network metrics and clinical test scores

Pearson correlation analysis was conducted between nodal strength in ROIs and clinical recognition test scores (with age, gender, and education as covariates). The partial correlation coefficient was listed in Table 4. Additionally, the mean functional connectivity strength of the NBS-based connected network exhibited a trend toward positive correlation with the AVLT cognitive recognition.

Discussion

Compared with common TLE cases, patients with non-lesional temporal lobe epilepsy (nl-TLE) do not show evidence of hippocampal sclerosis (HS) and always without distinct epileptogenic lesions in MRI examination, which will inevitably increase the difficulty for diagnosis and delay of the effective therapy. In this study, we aimed to find the disruption of functional connectivity in patients' white matter network. The results may serve as features in the diagnosis of nl-TLE.

In this study, white matter networks in both nl-TLE groups and HC group were found to have small-worldness. Besides, there was no significance found in the global clustering coefficient. This phenomenon indicates that the interconnectivity in the patients' networks is preserved to some extent, despite the alteration in the architecture of brain networks.

Compared with healthy controls' networks, significantly decreased global network efficiency and increased global shortest path length were observed in nl-TLE patients' networks. These two metrics measure the transform speed of information in the global network [20]. Thus, patients with nl-TLE may suffer a decline in the ability to combine

Table 4 Relationship between network metrics and clinical test scores in ROIs

Group	Brain region	Abbr.	Category	Partial correlation coefficient (*p* value)				
				MOCA	Boston Naming Test	DSST Exams	RAVLT recognition	RAVLT delayed recall
Right nl-TLE	Inferior frontal gyrus, orbital part	ORBinf.R	Paralimbic	0.296 (0.248)	− 0.139 (0.594)	0.255 (0.323)	0.371 (0.143)	0.556 (0.020)[a]
	Lingual gyrus	LING.R	Association	0.024 (0.928)	− 0.154 (0.555)	0.660 (0.004)[a]	0.526 (0.030)[a]	0.609 (0.010)[a]
	Supramarginal gyrus	SMG.L	Association	0.157 (0.546)	− 0.135 (0.607)	0.213 (0.413)	0.553 (0.021)[a]	0.681 (0.003)[a]
	Olfactory cortex	OLF.L	Limbic	0.682 (0.003)[a]	0.123 (0.639)	0.746 (0.001)[a]	0.612 (0.009)[a]	0.582 (0.014)[a]
	Middle occipital gyrus	MOG.L	Association	0.101 (0.701)	0.037 (0.889)	0.786 (< 0.001)[a]	0.464 (0.060)	− 0.150 (0.566)
	Temporal pole: middle temporal gyrus	TPOmid.L	Paralimbic	0.883 (< 0.001)[a]	0.564 (0.018)[a]	0.506 (0.038)[a]	0.510 (0.037)[a]	0.717 (0.001)[a]
	Amygdala	AMYG.L	Subcortical	0.676 (0.003)[a]	0.570 (0.017)[a]	0.547 (0.023)[a]	0.125 (0.632)	0.396 (0.115)
	Posterior cingulate gyrus	PCG.L	Paralimbic	− 0.130 (0.618)	0.496 (0.043)[a]	0.613 (0.009)[a]	0.588 (0.013)[a]	0.338 (0.185
	Amygdala	AMYG.R	Subcortical	0.651 (0.005)[a]	0.565 (0.018)[a]	0.492 (0.045)[a]	0.238 (0.357)	0.645 (0.005)[a]
Left nl-TLE	Inferior frontal gyrus, orbital part	ORBinf.R	Paralimbic	0.229 (0.452)	0.071 (0.818)	0.338 (0.259)	0.823 (0.001)[a]	0.707 (0.007)[a]
	Superior frontal gyrus, dorsolateral	SFGdor.L	Association	0.266 (0.379)	0.312 (0.299)	0.240 (0.430)	0.721 (0.005)[a]	0.580 (0.038)[a]
	Supramarginal gyrus	SMG.L	Association	− 0.061 (0.844)	− 0.311 (0.301)	0.432 (0.140)	0.578 (0.039)[a]	0.565 (0.044)[a]
	Lenticular nucleus, putamen	PUT.R	Subcortical	0.364 (0.221)	0.752 (0.003)[a]	0.624 (0.023)[a]	0.583 (0.036)[a]	0.863 (< 0.001)[a]
	Amygdala	AMYG.L	Subcortical	0.655 (0.015)[a]	0.665 (0.013)[a]	0.181 (0.554)	− 0.251 (0.409)	0.153 (0.619)
	Posterior cingulate gyrus	PCG.L	Paralimbic	0.009 (0.977)	− 0.187 (0.540)	0.490 (0.089)	0.429 (0.144)	0.597 (0.031)[a]

Partial correlation coefficient between mean nodal strength in ROIs and cognitive performance, using age, gender, and education as covariates

[a] Significant correlations ($p < 0.05$)

MOCA, Montreal Cognitive Assessment; *BNT*, Boston Naming Test; *DSST*, digit symbol substitution test; *RAVLT*, Rey Auditory Verbal Learning Test; *ROI*, region of interest

information rapidly, which can manifest as the cognitive impairment.

These findings are corresponding to the previous studies. A DTI study of children with localization-related epilepsy also showed increased path strength and declined global efficiency, with no significance found in the clustering coefficient [21].

In spite of the fact that no distinct lesion was found in nl-TLE patient groups, widespread changes in local network properties were observed. Consistent with previous studies [22, 23], our study indicates that patients with right nl-TLE have more extensive abnormalities than those of left nl-TLE. Thus, the two nl-TLE groups should be analyzed separately.

In both nl-TLE groups, the majority of nodes with decreased strength are distributed in the association regions, which receive rich information from multiple other brain regions [24]. Regions in this category such as superior temporal and frontal and parietal gyrus (STG, SFG, SPG) were reported in the previous TLE studies [25]. Reductions in regional connectivity may be a result of thinning in temporal and extratemporal cortical volumes in both TLE and nl-TLE patients. Structural alterations in these regions could lead to cognition impairment.

Abnormalities were also found in the amygdala (AMYG), right lingual gyrus (LING.R), and left middle occipital gyrus (MOG.L) in both nl-TLE groups. Amygdala is associated with the capability of memory consolidation [26]. Damages in the amygdala were also reported in the research of Bower et al in patients with temporal lobe epilepsy [27]. Lingual gyrus and middle occipital gyrus play an important role in the visual processing [26, 28]. Declined strength found in these two nodes may provide evidence for the disruption of the visual system in patients with nl-TLE.

More widespread abnormalities were found in the left posterior cingulate gyrus (PCG.L) and median cingulate and paracingulate gyri (DCG.R) in left nl-TLE, and middle temporal gyrus (TPOmid.L and TPOmid.R), left precentral gyrus (PreCG.L), and right Heschl gyrus (HES.R) in right nl-TLE. In respect of functional classification, nodes with declined strength in right nl-TLE mostly belong to the primary category. By contrast, altered nodes in left nl-TLE mainly belong to the paralimbic category, which is topologically isolated in the networks and has a relatively mild impact to the disruption of structural networks [24]. Such differences may explain the worse clinical behavior in the right nl-TLE group compared with the left nl-TLE group, which conforms to the results in a previous study.

In this study, nodes with significantly decreased strength were taken as ROIs. Then, correlation coefficients between the nodal strength and the cognition scores were estimated in those ROIs. Only a few nodes survived after the FWER correction. Nodal strength in ROIs was found to have an overall positive correlation with clinical parameters, indicating that the disruption in networks has a tendency to exacerbate the cognition impairment.

We noticed that the altered metrics specifically correlated with memory-related cognitive tests (RAVLT recognition and RAVLT delayed recall), which shows their potential to rate the severity of the disease. However, results become unstable when using cognitive tests covering many aspects (MOCA, Boston Naming Test, and DSST Exams). We speculate that several aspect-related brain regions were preserved from the structural disruption, and may conceal the performance of other aspects in those multi-aspect tests. Besides, several problems caused by cultural differences seem to lack consideration in the localization processing of these tests, which make patients confused about some questions.

Our study still has some limitations. Firstly, the computation of diffusion tensor tractography faces the common "fiber crossing" problem, which means the tracking procedure of diffusion tensor tractography will terminate when it comes to regions where the fiber is crossed and the FA values are low. In addition, we only discussed the regions where most of the nodal network properties show significant between-group differences and other regions which might have a correlation with nl-TLE have not been taken into consideration. Besides, the strict inclusion and exclusion criteria have resulted in the small sample size in this study, which makes the results remain to be further tested.

In this study, diffusion tensor tractography and graph theoretical analyses were used to investigate the alterations of WM network topological properties and structural connectivity in nl-TLE patients. The structural disruptions of networks were positively correlated with the clinical behavior, and were observed to be different in distribution and severity in the two nl-TLE groups. Our findings provide useful insights for the understanding of disease mechanisms of TLE and improving treatment outcomes for nl-TLE.

Funding The authors state that this work has not received any funding.

Compliance with ethical standards

Guarantor The scientific guarantor of this publication is Lan Chu.

Conflict of interest The authors of this manuscript declare no relationships with any companies, whose products or services may be related to the subject matter of the article.

Statistics and biometry One of the authors has significant statistical expertise.

Informed consent Written informed consent was obtained from all subjects (patients) in this study.

Ethical approval Institutional Review Board approval was obtained.

Methodology
- prospective
- diagnostic or prognostic study
- performed at one institution

References

1. Lin JJ, Salamon N, Lee AD et al (2007) Reduced neocortical thickness and complexity mapped in mesial temporal lobe epilepsy with hippocampal sclerosis. Cereb Cortex 17:2007–2018
2. Muhlhofer W, Tan YL, Mueller SG, Knowlton R (2017) MRI-negative temporal lobe epilepsy-what do we know? Epilepsia 58: 727–742
3. LoPinto-Khoury C, Sperling MR, Skidmore C et al (2012) Surgical outcome in PET-positive, MRI-negative patients with temporal lobe epilepsy. Epilepsia 53:342–348
4. Carne RP, O'Brien TJ, Kilpatrick CJ et al (2004) MRI-negative PET-positive temporal lobe epilepsy: a distinct surgically remediable syndrome. Brain 127:2276–2285
5. Helmstaedter C, Petzold I, Bien CG (2011) The cognitive consequence of resecting nonlesional tissues in epilepsy surgery–results from MRI- and histopathology-negative patients with temporal lobe epilepsy. Epilepsia 52:1402–1408
6. Tellez-Zenteno JF, Hernandez Ronquillo L, Moien-Afshari F, Wiebe S (2010) Surgical outcomes in lesional and non-lesional epilepsy: a systematic review and meta-analysis. Epilepsy Res 89: 310–318
7. Spencer SS (2002) Neural networks in human epilepsy: evidence of and implications for treatment. Epilepsia 43:219–227
8. Liao W, Zhang Z, Pan Z et al (2011) Default mode network abnormalities in mesial temporal lobe epilepsy: a study combining fMRI and DTI. Hum Brain Mapp 32:883–895
9. Bonilha L, Nesland T, Martz GU et al (2012) Medial temporal lobe epilepsy is associated with neuronal fibre loss and paradoxical increase in structural connectivity of limbic structures. J Neurol Neurosurg Psychiatry 83:903–909
10. Bonilha L, Helpern JA, Sainju R et al (2013) Presurgical connectome and postsurgical seizure control in temporal lobe epilepsy. Neurology 81:1704–1710
11. Liu M, Chen Z, Beaulieu C, Gross DW (2014) Disrupted anatomic white matter network in left mesial temporal lobe epilepsy. Epilepsia 55:674–682
12. McGorry PD, Yung AR, Phillips LJ (2003) The "close-in" or ultra high-risk model: a safe and effective strategy for research and clinical intervention in prepsychotic mental disorder. Schizophr Bull 29:771–790
13. Whelan CD, Alhusaini S, O'Hanlon E et al (2015) White matter alterations in patients with MRI-negative temporal lobe epilepsy and their asymptomatic siblings. Epilepsia 56:1551–1561
14. Mori S, Crain BJ, Chacko VP, van Zijl PC (1999) Three-dimensional tracking of axonal projections in the brain by magnetic resonance imaging. Ann Neurol 45:265–269
15. Tzourio-Mazoyer N, Landeau B, Papathanassiou D et al (2002) Automated anatomical labeling of activations in SPM using a macroscopic anatomical parcellation of the MNI MRI single-subject brain. Neuroimage 15:273–289
16. Rubinov M, Sporns O (2010) Complex network measures of brain connectivity: uses and interpretations. Neuroimage 52:1059–1069
17. Watts DJ, Strogatz SH (1998) Collective dynamics of 'small-world' networks. Nature 393:440–442
18. Wang J, Wang X, Xia M, Liao X, Evans A, He Y (2015) GRETNA: a graph theoretical network analysis toolbox for imaging connectomics. Front Hum Neurosci 9:386
19. Latora V, Marchiori M (2001) Efficient behavior of small-world networks. Phys Rev Lett 87:198701
20. Widjaja E, Zamyadi M, Raybaud C, Snead OC, Doesburg SM, Smith ML (2015) Disrupted global and regional structural networks and subnetworks in children with localization-related epilepsy. AJNR Am J Neuroradiol 36:1362–1368
21. Lemkaddem A, Daducci A, Kunz N et al (2014) Connectivity and tissue microstructural alterations in right and left temporal lobe epilepsy revealed by diffusion spectrum imaging. Neuroimage Clin 5:349–358
22. Scanlon C, Mueller SG, Cheong I, Hartig M, Weiner MW, Laxer KD (2013) Grey and white matter abnormalities in temporal lobe epilepsy with and without mesial temporal sclerosis. J Neurol 260: 2320–2329
23. Mueller SG, Laxer KD, Barakos J, Cheong I, Garcia P, Weiner MW (2009) Widespread neocortical abnormalities in temporal lobe epilepsy with and without mesial sclerosis. Neuroimage 46:353–359
24. Achard S, Salvador R, Whitcher B, Suckling J, Bullmore E (2006) A resilient, low-frequency, small-world human brain functional network with highly connected association cortical hubs. J Neurosci 26:63–72
25. Shu N, Liu Y, Li K et al (2011) Diffusion tensor tractography reveals disrupted topological efficiency in white matter structural networks in multiple sclerosis. Cereb Cortex 21:2565–2577
26. Blair HT, Schafe GE, Bauer EP, Rodrigues SM, LeDoux JE (2001) Synaptic plasticity in the lateral amygdala: a cellular hypothesis of fear conditioning. Learn Mem 8:229–242
27. Bower SP, Vogrin SJ, Morris K et al (2003) Amygdala volumetry in "imaging-negative" temporal lobe epilepsy. J Neurol Neurosurg Psychiatry 74:1245–1249
28. Price CJ, Wise RJ, Watson JD, Patterson K, Howard D, Frackowiak RS (1994) Brain activity during reading. The effects of exposure duration and task. Brain 117(Pt 6):1255–1269